

**RESPONSES TO REVIEWERS COMMENTS FOR BG-2018-448 by Lorenzo et al. 3<sup>rd</sup> resubmission**

---

**Referee #1**

**Review comments for “Particulate trace metal dynamics in response to increased CO<sub>2</sub> and iron availability in a coastal mesocosm experiment”.**

**The authors have improved this manuscript with addressing my comments. My serious concern is mostly resolved. However, the authors did not resolve all of my concerns. I still find several points which need to be improved before publication.**

**I have read this version of manuscript carefully, and I still feel that explanation of statistically analysis for Table 1 is not kind for reader. Why author do not describe following information in the text or caption of Table 1?<sup>[1]</sup><sub>SEP</sub> “We used all the days because we performed a Split-Plot ANOVA (or mixed model) which integrates fixed factors (Co<sub>2</sub> and Fe) and a repeated measures factor (time) by using the posthoc Bonferroni, saying that the statistical treatment was a split-plot ANOVA+Bonferroni, compulsory means that time was fully considered during the whole experimental period.”**

**They have made the response only to reviewer’s comments. This information is very important for reader’s understanding that how the statistically analysis have done.**

Thanks for the comment. It has been included now as follows:

*“Table 1. Statistical analyses (Split-plot ANOVA) of the effects of high CO<sub>2</sub>, the addition of DFB, and their interaction, as well as the effect of time, on the concentrations of particulate metals (mmol L<sup>-1</sup>, data in Table S2, and Figure 3) in particles collected from the different mesocosms treatments. We used all the days for the analyses because the Split-Plot ANOVA integrates fixed factors (CO<sub>2</sub> and Fe) and a repeated measures factor (time) by using the post-hoc Bonferroni, thus, time was fully considered during the whole experimental period.”*

**Line 125 “By day 17,.....and/or the addition of DFB (Chen et al., 2004).” Increased dissolved Fe by adding DFB is bioavailable?**

DFB enhances Fe solubility (Chen et al. 2004), which increases the dFe pool. Given the positive response of *E. huxleyi* growth in the low CO<sub>2</sub>, high DFB treatments, the DFB seems to have improved the bioavailability of Fe to *E. huxleyi*. This is supported by previous studies showing that *E. huxleyi* produces a wide range of compounds with high affinity for Fe (Boye & Van den Berg 2000). Furthermore, *E. huxleyi* is able to acquire Fe from a variety of organic Fe complexes (Hartnett et al. 2012), including Fe-DFB (Shaked & Lis 2012, Lis et al. 2015).

This has been clarified in the first paragraph of the discussion, although it was also amended around Ln 125.

**Is DFB-Fe can be detected by CL-FIA which described in Segovia et al., 2017? Strong chelate like DFB prevent dissolved Fe detection measuring by resin preconcentrate-CL-FIA measurement system. It should be made clear that which chemical species do**

**authors describe as for dissolved Fe in this study (Is DFB-bounded Fe included in this dissolved fraction, or not?). Also, it is necessary to clearly describe how do authors think about that how the availability of iron was changed by adding DFB.**

We have included the following paragraph for clarification in the text, Ln 147-153:

*“The pH of the 0.2 µm filtered DFe samples was lowered to 1.7 (using SeaStar® HCl) upon collection. Lowering the pH to 1.7, with HCl for more than 24 hours, ensures solubilisation of all the Fe in the sample, as well as the release of all the Fe bound within strong organic complexes (such as Fe-DFB), thus making all DFe available for analysis (Johnson et al. 2007). During flow-injection analysis with chemiluminescence detection (FIA-CL), the sample is only buffered to a higher pH immediately before entering the flow cell, right in front of the photomultiplier; so that Fe-DFB complexing kinetics are sufficiently slow to allow total DFe to be measured”*

Johnson et al. 2007. Developing Standards for Dissolved Iron in Seawater. EOS Transactions American Geophysical Union 88 (11): p. 131-132

**Some previous studies indicate that DFB-bounded Fe is not available, as authors described in the text. Is DFB-Fe available for E. Huxley? If so, please indicate a reference. Or, do adding DFB induce other chemical species of dissolved fraction? Author should describe this aspect clear, because this point is very important for this study.**

Reviewer is right. This is a crucial point. The following clarification has been inserted in the text in Lns 264-268:

*“Our results suggest that E. huxleyi is able to utilise DFB-bound Fe (Fe-DFB) due to the dynamics observed in Segovia et al. 2017. Indeed, E. huxleyi has been shown to produce a wide range of metabolites which are organic complexes with high affinity for Fe (Boye & Van den Berg 2000), and, E. huxleyi is also able to acquire Fe from organic Fe complexes (Hartnett et al. 2012) including Fe-DFB (Shaked & Lis 2012, Lis et al. 2015)”*

**Line 130-132, “Water samples from.....onshore laboratory.” This sentence should be moved in section 2.3.1.**

We are not taking this suggestion because section 2.3.1 only refers to pMe sampling. The paragraph reviewer refers to concern to all variable samplings, not only pMe.

**Authors should indicate manufacture and model information for the “vacuum pump”.**

Included in Ln 132:

*“...pumping of 25 L volume into acid-washed carboys by using membrane vacuum pumps (PALL) working at reverse flow. Carboys were quickly transported...”*

**Line 145, “for this very experiment.”. What is “very”.**

“Very” means “the same”. Grammar is correct.

**Line 155, Authors should indicate the type of “Filters”. Is this also AcroPac Supore, but membrane type?? Size??**

It has been specified as follows:

*“Seawater was collected from each mesocosm, filtered through AcroPak® capsule filters with 0.2 µm Supor® membrane into the trace metal clean LDPE bottles”.*

**Line 158, “without manipulation” should be changed to “without oxalate-EDTA wash”.  
Line 164, Authors should indicate material and volume of “centrifuge tubes”**

Added:

*“...directly to 2 mL centrifuge polypropylene tubes for storage...”*

**Line 178, blank value should be appeared in the Supplemental material such as S-Table 1.**

As indicated in the Materials and Methods “Filter blanks were collected and subjected to the same storage, digestion, dilution, and analysis processes, and these blank values were subtracted from sample measurements” These filters blanks were collected every time we collected samples, and the samples collected in a given day were corrected with the value of the blanks collected that same day. Thus, it is practically impossible for us to include the blanks for all these measurements in Supplementary Table 1. They were inherently included!

While writing our manuscript, we also searched similar particulate metal manuscripts and we reported the data as reported in those manuscripts. The blanks are not reported in the data tables, as the data are corrected already for them (e.g. Cid et al. 2012, *J Oceanogr.* 68:985–1001; Ohnemus and Lam 2012, [\*Deep Sea Research Part II: Topical Studies in Oceanography\* 116: 283-302](#); Ho et al. 2007, *Limnol. Oceanogr.*, 52(5): 1776–1788).

In light of this, we think our data are correct in the present form.

**Line 215-216, “This diatom bloom was associated with a sharp decrease in nitrate and silicate acid concentration”. I think this is not correct. Why nitrate decrease with diatom decreasing? Silicate have not sharp decreased during diatom decreasing.**

Silicate was first consumed. When we measured day 0 and day 1, silicate was already gone. Then nitrate was consumed. Iron requirements of phytoplankton are strongly influenced by the availability and source of nitrogen (Maldonado and Price 1996, Schoffmann et al. 2016). Phytoplankton that is utilizing nitrate ( $\text{NO}_3^-$ ) has higher Fe requirements than phytoplankton utilizing ammonium ( $\text{NH}_4^+$ ) for growth (Maldonado and Price 1996, Schoffmann et al. 2016).  $\text{NH}_4^+$  can be directly incorporated into amino acids, while extra iron is needed for nitrate assimilation, because nitrate and nitrite reductase contain Fe cofactors. In addition, the energy for  $\text{NO}_3^-$  reduction is produced by the Fe-rich photosynthetic electron transport chain. Thus  $\text{NO}_3^-$  was consumed by other phytoplankton groups not limited by Fe harming diatoms that were already silicate limited.

This is clearly explained in Segovia et al.,2017 so we refer to our paper for further details.

**Line 327, “Figure 4” should be changed “Figure 3”.**

Done

**429-430, “promoted a massive bloom of E huxley in the treatment with ambient CO<sub>2</sub>, due to increased dissolved Fe”. It should be made clear that which chemical species do authors describe as for dissolved Fe in this study (Is DFB-bounded Fe included in this dissolved fraction, or not?). Some previous studies indicate that DFB-bounded Fe is not available, as authors described in the text. Is DFB-Fe available for E. Huxley? If so, please indicate reference. See comment above too.**

This has been answered before.

**Line 435-436, “The decrease in particulate Fe may..... in open ocean setting.”. Delete this sentence. This is not a conclusion from this study. No data from this study indicate this.**

Done

**End of review.**

-----

We thank the reviewers for their constructive comments and their time, and we hope that our responses are satisfactory

Yours sincerely,

Maria Segovia and Maite Maldonado

**Particulate trace metal dynamics in response to increased CO<sub>2</sub> and iron availability in a coastal mesocosm experiment**

M. Rosario Lorenzo<sup>1</sup>, María Segovia<sup>1</sup>, Jay T. Cullen<sup>2</sup>, and María T. Maldonado<sup>3</sup>

<sup>1</sup>Department of Ecology, Faculty of Sciences, University of Málaga, Bulevar Louis Pasteur s/n, 29071-Málaga, Spain

<sup>2</sup>School of Earth and Ocean Sciences, University of Victoria, 3800 Finnerty Road, A405, Victoria BC V8P 5C2

Canada

<sup>3</sup>Department of Earth, Ocean and Atmospheric Sciences, University of British Columbia, 2207 Main Mall, Vancouver

BC V6T 1Z4, Canada

*Correspondence to:* María Segovia (segovia@uma.es) and María T. Maldonado (mmaldonado@eoas.ubc.ca)

**Abstract.** Rising concentrations of atmospheric carbon dioxide are causing ocean acidification and will influence marine processes and trace metal biogeochemistry. In June 2012, in Raunefjord (Bergen, Norway) we performed a mesocosm experiment, comprised of a fully factorial design of ambient and elevated  $p\text{CO}_2$  and/or an addition of the siderophore desferrioxamine B (DFB). In addition, the macronutrient concentrations were manipulated to enhance a bloom of the coccolithophore *Emiliania huxleyi*. We report here the changes in particulate trace metal concentrations during this experiment. Our results show that particulate Ti and Fe were dominated by lithogenic material while particulate Cu, Co, Mn, Zn, Mo and Cd had a strong biogenic component. Furthermore, significant correlations were found between particulate concentrations ( $\text{mol L}^{-1}$ ) of Cu, Co, Zn, Cd, Mn, Mo, and P in seawater and phytoplankton biomass ( $\mu\text{gC L}^{-1}$ ), supporting a significant influence of the bloom in the distribution of these particulate elements. The concentrations of these biogenic metals ( $\text{mol L}^{-1}$ ) in the *E. huxleyi* bloom were ranked as:  $\text{Zn} > \text{Cu} \approx \text{Mn} > \text{Mo} > \text{Co} > \text{Cd}$ . Changes in  $\text{CO}_2$  affected total particulate concentrations ( $\text{mol L}^{-1}$ ) and biogenic metal ratios (Me:P) for some metals, while the addition of DFB only affected significantly the concentrations of some particulate metals ( $\text{mol L}^{-1}$ ). Variations in  $\text{CO}_2$  had the most clear, and significant effect on particulate Fe concentrations ( $\text{mol L}^{-1}$ ), decreasing its concentration under high  $\text{CO}_2$ . Indeed, high  $\text{CO}_2$  and/or DFB promoted the dissolution of particulate Fe, and the presence of this siderophore helped maintaining high dissolved Fe. This shift between particulate and dissolved Fe concentrations, in the presence of DFB, promoted a massive bloom of *E. huxleyi* in the treatments with ambient  $\text{CO}_2$ . Furthermore, high  $\text{CO}_2$  decreased the Me:P ratios of Co, Zn and Mn, while increased the Cu:P ratios. These findings support theoretical predictions that the Me:P ratios of metals whose seawater dissolved speciation is dominated by free ions (e.g. Co, Zn and Mn) will likely decrease or stay constant under ocean acidification. In contrast, high  $\text{CO}_2$  is predicated to shift the speciation of dissolved metals associated with carbonates, such as Cu, increasing their bioavailability, and resulting in higher Me:P ratios.

**Key words:** Global change, Fe,  $\text{CO}_2$ , particulate trace metals, dissolved trace metals, mesocosms, *Emiliania huxleyi*, phytoplankton

Con formato: Español

Con formato: Español

Con formato: Español

Con formato: Español

Con formato: Español

Con formato: Español

Con formato: Español

Con formato: Español

## 1. Introduction

Marine phytoplankton contribute half of the world's total primary productivity, sustaining marine food webs and driving the biogeochemical cycles of carbon and nutrients (Field et al., 1998). Annually, phytoplankton incorporate approximately 45 to 50 billion metric tons of inorganic carbon (Field et al., 1998), removing a quarter of the CO<sub>2</sub> emitted to the atmosphere by anthropogenic activities (Canadell et al., 2007). Yet, the atmospheric CO<sub>2</sub> concentration has increased by 40 % since pre-industrial times as a result of anthropogenic CO<sub>2</sub> emissions, producing rapid changes in the global climate system (Stocker et al., 2013). The dissolution of anthropogenic CO<sub>2</sub> in seawater, causes shifts in the carbonate chemical speciation, and leads to ocean acidification (OA). Marine ecosystems are sensitive to changes in pH because pH strongly affects chemical and physiological reactions (Hoffman et al., 2012). Increased CO<sub>2</sub> in seawater may enhance or diminish phytoplankton productivity (Mackey et al., 2015), decrease the CaCO<sub>3</sub> production in most planktonic calcifiers (Riebesell and Tortell 2011), and/or inhibit organic nitrogen and phosphorus acquisition (Hutchins et al., 2009). Thus, the biogeochemical cycling of nutrients is predicted to be highly affected by OA (Hutchins et al. 2009), as well as the distribution and speciation of trace metals in the ocean (Millero et al., 2009).

Trace metals, including Fe, Zn, Mn, Cu, Co and Mo, are essential for biological functions (e.g. photosynthesis, respiration and macronutrient assimilation), and Cd can supplement these functions. Trace metals availability can influence phytoplankton growth and community structure (Morel and Price, 2003). In turn, plankton control the distribution, chemical speciation, and cycling of trace metals in the sea (Sunda, 2012), by, for example, releasing organic compounds that dominate the coordination chemistry of metals, internalizing trace elements into the cells, and reducing and/or oxidizing metals at the cell surface. The chemistry of redox speciation of active trace metals is highly dependent on pH. Fe occurs in two main redox states in the environment: oxidized ferric Fe (Fe (III)), which is poorly soluble at circumneutral pH; and reduced ferrous Fe (Fe (II)), which is more soluble in natural seawater, but becomes rapidly oxidized (Millero et al. 1987). Fe speciation and bio-availability are dynamically controlled by the prevalent changing redox conditions. Also, as the ocean becomes more acidic, reduction of Cu (II) will increase, as the ionic form of Cu (II) is reduced to Cu (I) (Millero et al., 2009). The effect of higher concentrations of Cu (I) in surface waters on biological systems is not well known. Therefore, while the effects of OA on inorganic metal speciation will be more pronounced for metals that form strong complexes with carbonates (e.g. copper) or hydroxides (e.g. Fe and aluminium), those that form stable complexes with chlorides (e.g. cadmium) will not be greatly affected. pH mediated changes in concentrations and/or speciation could possibly enhance trace metals limitation and/or toxicity to marine plankton (Millero et al., 2009).

Fe is crucial for phytoplankton growth because it is involved in many essential physiological processes, such as photosynthesis, respiration, and nitrate assimilation (Behrenfeld and Milligan, 2013). The decrease in seawater pH in response to OA may increase Fe solubility (Millero et al., 2009), but it may also result in unchanged or lower Fe bioavailability, depending on the nature of the strong organic Fe ligands (Shi et al., 2010). Consequently, changes in Fe bioavailability due to ocean acidification can affect positively or negatively ocean productivity and CO<sub>2</sub> drawdown. Copper is an essential micronutrient but may be toxic at high concentrations (Semeniuk et al., 2016). An increase in free cupric ion concentrations in coastal areas due to ocean acidification (Millero et al., 2009) could result in negative effects on phytoplankton. Given that trace metals are essential for phytoplankton productivity, and that they are actively internalized during growth, it is important to study the impacts of ocean acidification on the trace metal content of ecologically significant plankton species.

In a rapidly changing global environment, generated by anthropogenic CO<sub>2</sub> emissions, it is critical to gain adequate

83 understanding about ecosystem responses. Due to the complex interactions in aquatic ecosystems, such predictions have  
84 so far not been possible to do based upon observational data and modelling alone. However, direct empirical studies on  
85 natural communities offer a robust tool to analyse interactive effects of multiple stressors. Specifically, mesocosm  
86 experiments allow perturbation studies with a high degree of realism compared to other experimental systems such as in  
87 the laboratory (high controlled conditions usually far from reality) or *in situ* in the ocean (where not all the interactions  
88 are contemplated) (Riebesell et al., 2010, Stewart et al., 2013, Riebesell and Gatusso, 2015).

90 In the present work a bloom of the coccolithophorid *Emiliana huxleyi* was induced in a mesocosm experiment in a  
91 Norwegian fjord, where the speciation of particulate and dissolved trace metals is very dynamic (e.g. Fe; Ozturk et al.  
92 2002). We aimed to examine and characterize the change of particle trace metals during an *E. huxleyi* bloom under the  
93 interactive effects of increased CO<sub>2</sub> and/or dissolved Fe. *Emiliana huxleyi* is the most cosmopolitan and abundant  
94 coccolithophore in the modern ocean (Paasche, 2002) and its growth and physiology has been studied under this  
95 experimental conditions (Segovia et al., 2017, Segovia et al., 2018, Lorenzo et al., 2018). Furthermore, *E. huxleyi* has  
96 unique trace metal requirements relative to other abundant phytoplankton taxa (ie. diatoms or dinoflagellates; Ho et al.  
97 2003). Coccolithophores play a key role in the global carbon cycle because they produce photosynthetically organic  
98 carbon, as well as particulate inorganic carbon through calcification. These two processes foster the sinking of  
99 particulate organic carbon—and trace metals—and contribute to deep ocean carbon export (Hutchings, 2011) and  
100 ultimately to organic carbon burial in marine sediments (Archer, 1991, Archer and Maier-Reimer., 1994). However,  
101 ocean acidification will disproportionately affect the abundance of coccolithophores, as well as their rates of  
102 calcification and organic carbon fixation (Zondervan et al., 2007). The aim of the present study was to characterize the  
103 changes in particulate trace metal concentrations—in both lithogenic and biogenic particles— during a bloom of  
104 *E. huxleyi* under realistic changes in CO<sub>2</sub> and Fe bioavailability expected by 2100.

## 107 2. Materials and methods

### 108 2.1 Experimental set-up

109 The experimental work was carried out in June 2012 in the Raunefjord, off Bergen, Norway as described in detail by  
110 Segovia et al., (2017). Twelve mesocosms (11 m<sup>3</sup> each) were set-up in a fully factorial design with all combinations of  
111 ambient and elevated pCO<sub>2</sub> and dFe in three independent replicate mesocosms. The mesocosms were covered by lids  
112 (both transparent to PAR and UVR) and filled with fjord water from 8 m depth. We achieved two CO<sub>2</sub> levels  
113 corresponding to present (390 ppm, LC) and those predicted for 2100 (900 ppm, HC) by adding different quantities of  
114 pure CO<sub>2</sub> gas (Schulz et al., 2009). The specific CO<sub>2</sub> concentration and the CO<sub>2</sub> inlet flows in the mesocosms were  
115 measured by non-dispersive infrared analysis by using a Li-Cor (LI-820) CO<sub>2</sub> gas analyser (Li-COR, Nebraska, USA).  
116 CO<sub>2</sub> concentrations in the mesocosms were calculated from pH and total alkalinity measurements using the CO<sub>2</sub> SYS  
117 software (Robbins et al., 2010). At the beginning of the experiment, nitrate (10 µM final concentration) and phosphate  
118 (0.3 µM final concentration) were added to induce a bloom of the coccolithophore *Emiliana huxleyi*, according to Egge  
119 & Heimdal (1994). Following recommendations by Marchetti and Maldonado (2016), to induce changes in Fe  
120 availability, and analyse its effects on the plankton community, 70 nM (final concentration) of the siderophore  
121 desferrioxamine B (DFB) (+DFB and -DFB treatments) (Figure S1b-supplemental material) was added to half of the  
122 mesocosms on Day 7, when the community was already acclimated to high CO<sub>2</sub>. The initial dFe concentration before  
123 DFB addition was about 4.5 nM. Even though DFB is a strong Fe-binding organic ligand often used to induce Fe  
124 limitation in phytoplankton (Wells 1999), DFB additions may also increase the dissolved Fe pool in environments  
125 with high concentrations of colloidal and/or particulate Fe, such as fjords (Kuma et al. 1996, Öztürk et al. 2002). By day

126 17, dissolved Fe concentrations were significantly higher (by ~3-fold) in the high CO<sub>2</sub> and DFB treatments than in the  
127 control (Segovia et al. 2017). These results support an increase in the solubility of Fe in seawater by either lowering its  
128 pH (Millero 1998; Millero et al. 2009) and/or the addition of DFB (Chen et al. 2004). The multifactorial experimental  
129 design consisted of triplicate mesocosms per treatment and the combinations of high and ambient pCO<sub>2</sub> and dFe levels,  
130 resulted in a total of 12 mesocosms: LC-DFB (control), LC+DFB, HC+DFB and HC-DFB. Water samples from each  
131 mesocosm were taken from 2 m depth by gentle vacuum pumping of 25 L volume into acid-washed carboys by using  
132 membrane vacuum pumps (PALL) working at reverse flow. Carboys were quickly transported to the onshore  
133 laboratory. The biological and chemical variables analysed were phytoplankton abundance and species composition,  
134 dissolved Fe and Cu concentrations (dFe, dCu), nutrient concentrations (nitrate, phosphate, silicic acid and ammonium)  
135 and particulate trace metal concentrations.

136  
137 **2.2 Dissolved copper (dCu)**

138 Low density polyethylene (LDPE) bottles were cleaned with 1% alkaline soap solution for one week, then filled with 6  
139 M trace metal grade HCl (Seastar, Fisher Chemicals) and submerged in a 2 M HCl bath for one month. For transport,  
140 they were filled with 1 M trace metal grade HCl for one more month and kept double bagged. In between each acid  
141 treatment, the bottles were rinsed with Milli-Q water (Millipore; hereafter referred to as MQ). Before sampling, the  
142 bottles were rinsed three times with filtered seawater. Seawater was collected from each mesocosm, filtered through  
143 AcroPak® capsule filters with 0.2 µm Supor® membrane, into the trace metal clean LDPE bottles, and acidified with  
144 ultra-clean trace metal grade HCl in a Class 100 laminar flow hood. Total dissolved Cu concentrations were measured  
145 following Zamzow et al., (1998) using a flow injection analysis chemiluminescence detection system (CL-FIA,  
146 Waterville Analytical). Total dissolved Fe concentrations were measured as described in Segovia et al., (2017) for this  
147 very experiment. The pH of the 0.2 µm filtered dFe samples was lowered to 1.7 by using SeaStar HCl upon collection.  
148 Lowering the pH to 1.7, with HCl for more than 24 hours, ensures solubilisation of all the Fe in the sample, as well as  
149 the release of all the Fe bound within strong organic complexes (such as Fe-DFB), thus making all dFe available for  
150 analysis (Johnson et al. 2007). During (FIA-CL, the sample is only buffered to a higher pH immediately before entering  
151 the flow cell, right in front of the photomultiplier; so that Fe-DFB complexing kinetics are sufficiently slow to allow  
152 total dFe to be measured.

153  
154  
155 **2.3 Particulate metals (pMe)**  
156 **2.3.1 Sampling**

157 All equipment and sampling material used during this study was rigorously acid-washed under trace metal clean  
158 conditions and protocols according to GEOTRACES . The material was cleaned with Milli-Q water (MQw) with 10 %  
159 Extran (Fisher Chemicals) at 60°C for 6h, followed by 3 thorough rinses with MQw at room T. The material was then  
160 cleaned with 10 % HPLC grade HCl (Sigma-Aldrich) at 60°C or 12h and then rinsed thoroughly 5 times with MQw at  
161 room T. The material was then covered by plastic and transported to the raft. Sampling in the raft was carried out under  
162 a mobile plastic cover hood. Filters were precleaned with 10% trace metal grade hydrochloric acid (Seastar, Fisher  
163 Chemicals), at 60°C overnight and were rinsed with MQw. Seawater samples (1-3.5 L) were filtered gently onto 0.45  
164 µm acid washed Supor ®-450 filters (within a trace metal clean Swinnex filter holder) on days 12, 17 and 21 of the  
165 experiment. Four technical replicates were taken from each mesocosm. Two filters were analysed without oxalate-  
166 EDTA wash and the other two were individually washed with oxalate-EDTA reagent to remove extracellular Fe, as  
167 well as other metals (Tang and Morel, 2006). Immediately following filtration, the treated filters were soaked with 20

Eliminado: at  
Eliminado: that

Con formato: Interlineado: 1.5 líneas

Eliminado: 0.2 µm  
Eliminado: capsule filters

Con formato: Fuente: 10 pto, Sin Cursiva, Inglés (americano)  
Con formato: Fuente: 10 pto, Sin Cursiva  
Con formato: Fuente: 10 pto, Sin Cursiva, Inglés (americano)  
Con formato: Fuente: 10 pto, Sin Cursiva  
Con formato: Fuente: 10 pto, Sin Cursiva, Inglés (americano)  
Con formato: Fuente: 10 pto, Sin Cursiva, Inglés (americano)  
Con formato: Fuente: 10 pto, Sin Cursiva, Inglés (americano)  
Con formato: Fuente: 10 pto, Sin Cursiva, Inglés (americano)  
Con formato: Inglés (americano)

Eliminado: manipulation



173 mL EDTA–oxalate solution, added to the headspace of the Swinnex holders, with an acid-washed polypropylene  
174 syringe. After 10 min, vacuum was applied to remove the oxalate solution and 10 mL of 0.2 µm filtered chelexed  
175 synthetic oceanic water (SOW) solution was passed through the filter to rinse off any remaining oxalate solution.  
176 Replicate filters that were not treated with oxalate solution were transferred directly to [2 mL centrifuge polypropylene](#)  
177 tubes for storage. The filters with particles were frozen in acid-washed 2 mL polypropylene tubes and then, dried and  
178 stored until analysis.

179

### 180 2.3.2 Analytical methods

181 Filters were digested in 7-mL acid-washed Teflon (Teflon, Rochester, NY, USA) vials. Teflon vials were also  
182 precleaned using 10% trace metal hydrochloric acid (Fisher, trace metal grade) during two days and then, with nitric  
183 acid (Fisher, trace metal grade) at 70 °C during three days. In between each acid treatment, the bottles were rinsed with  
184 MQ. Samples were digested in 3 mL of HNO<sub>3</sub> and 0.5 mL of HF (Fisher, trace metal grade) with lids on for 1 h on a  
185 hot plate at 200 °C. The lids were then removed to evaporate HF at 200°C. After this, 1.5 mL of HNO<sub>3</sub> were added and  
186 the samples were heated with lids on overnight at 150 °C. Finally, 2.25 mL of HClO<sub>4</sub> (Fisher, Optima grade) were  
187 added and the samples were heated for 4 h at 200 °C. After complete digestion, the samples were dried on hot plates at  
188 200°C. The dried samples were dissolved in 1% nitric acid with 1 ppb in internal standard. The analysis was performed  
189 using a high-resolution inductively coupled plasma-mass spectrometer (ICP-MS, Element XR, Thermo Scientific) and  
190 the described instrumental settings (Table S1). Filter blanks were collected and subjected to the same storage, digestion,  
191 dilution, and analysis processes, and these blank values were subtracted from sample measurements. Particulate  
192 samples for ICP-MS analysis were processed in a trace metal-clean laboratory under a trace metal-clean laminar flow  
193 fume hood.

194

### 195 2.3.3 The effect of oxalate-EDTA wash on particulate trace metal concentrations

196 To better estimate the biogenic fraction of the particulate metals, the filters were washed with an oxalate-EDTA  
197 solution, which removes extracellular metals and oxyhydroxides (Tovar-Sanchez et al., 2003; Tang and Morel, 2006).  
198 In our study, the oxalate wash significantly decreased the concentration of all particulate metals, with the exception of  
199 Al and Ti (Tables S2 and S3), as observed by Rauschenberg and Twining (2015). The quantity of metal remaining after  
200 the oxalate wash (i.e. biogenic fraction) varied among elements (Tables S2 and S3). In general, the concentrations of Fe  
201 and Co in the particles were decreased the least by the oxalate wash by ~ 25%, while Mo and Pb concentrations were  
202 decreased the most by ~70%. The concentrations of particulate Cu, Zn, Cd and Mn were reduced by 50% by the oxalate  
203 wash. As shown previously (Sanudo-Wilhelmy et al. 2004), the oxalate reagent also removed extracellular P (by ~20%,  
204 Table S2 & S3). Compared to Rauschenberg and Twining (2015), the estimates of the biogenic fraction, after the  
205 oxalate wash, were in agreement for Co, Cu and P, and lower for Fe, Mn, Zn and Cd concentrations.

206

207 However, the efficacy of the oxalate wash to dissolve Fe, and other metals, from lithogenic particles is not well  
208 constrained (Frew et al. 2006, Rauschenberg and Twining., 2015, King et al., 2012). Therefore, the results obtained  
209 after the oxalate-EDTA wash should be interpreted with caution because we do not know whether the removed metal  
210 fraction is a) only lithogenic; b) mainly lithogenic but some biogenic fraction is also removed, or c) whether metals  
211 absorbed onto particles are equally labile to the wash on biogenic and lithogenic particles. Given that many of the  
212 trends we observed were identical for the oxalate-EDTA washed and non-washed particles [i.e. higher Me  
213 concentrations in the LC+DFB treatments (Table S2 & S3) and positive correlations between phytoplankton biomass  
214 and Me concentrations (Lorenzo-Garrido 2016)], below we present and discuss only the non-oxalate wash results.

215

## 216 2.4 Statistical analyses

217 Data were checked for normality (by Shapiro-Wilks' test), homoscedasticity (by Levene's test) and sphericity (by  
218 Mauchly's test). All data met the requirements to perform parametric tests. Statistical significance of treatment effects  
219 was carried out using Split-Plot ANOVA followed by post-hoc Sidak and Bonferroni tests (considering  $P < 0.05$  as  
220 significant). All analyses were performed using the General Linear Model (GLM) procedure. The correlation between  
221 variables was analysed by Pearson's product-moment multiple comparisons (considering  $P < 0.05$  as significant).  
222 Statistical analyses were carried out using SPSS v22 (IBM statistics) and Sigmaplot 12 (Systat Software, Chicago,  
223 USA).

## 225 3. Results

### 226 3.1 Biological and chemical characteristics during the bloom

227 Plankton community dynamics and their response to the applied treatments in the mesocosms are described in detail by  
228 Segovia *et al.* (2017). Briefly, at the beginning of the experiment (days 1-10) a bloom of large chain-forming diatoms  
229 was observed, which declined by day 7 (Figure S1g- supplemental material). This diatom bloom [decline](#) was  
230 associated with a sharp decrease in nitrate and silicic acid concentrations (Figure S2-supplemental material, [see Segovia](#)  
231 [et al., 2017 for further details](#)). Picoeukaryotes, dominated the phytoplankton community on day 8 (Figure S1d).  
232 During the first 10 days of the experiment, there were no significant differences in the chemical variables measured  
233 between the treatments (Figures S3 and S2 -supplemental material). On day 7, half of the mesocosms were amended by  
234 adding DFB (+DFB treatments). Between day 7 and 17, an increase in dFe was observed in all treatments, except in the  
235 control (Figure S3). This increase in dFe was sustained for the entire experiment in the DFB treatments (Figure S3).  
236 Dissolved Cu concentrations were not affected by the different treatments (Figure S3). After day 10, a massive bloom  
237 of the coccolithophore *E. huxleyi* developed under LC +DFB condition (Figure S1b), out-competing the rest of the  
238 plankton groups (Figure S1). This bloom was not observed either in the control treatment (LC-DFB) or in the HC  
239 treatments, although *E. huxleyi* was still the most abundant species in all treatments; with the exception of the HC-DFB  
240 treatment (Figure S1b).

### 242 3.2 Particulate metal concentrations during the mesocosm experiment

243 The pMe concentrations (nM, mean of all treatments and dates) during the experiment were highest for Al, Fe and Zn,  
244 and lowest for Cd, following this trend:  $Al \approx Fe \approx Zn > Ti > Cu \approx Mn > Mo \approx Pb > Co > Cd$  (Figure 1, Table S2).  
245 Significant changes over time were observed for all particulate trace metal concentrations (Fe, Cu, Co, Zn, Cd, Mn, Mo  
246 and Pb), except for Ti and Al (Figure 1, Table 1). The only metal that showed a significant time-dependent decrease in  
247 its particulate concentration was Fe (Figure 1, Table 1). In general, the treatments with the highest particulate metals  
248 concentrations also exhibited the highest particulate P, except for Al, Ti, Fe, and Pb (Figure 1, Table S2). On days 12  
249 and 17, the highest particulate metals concentrations were observed in the LC+DFB treatment, while on day 21, they  
250 were observed in both LC treatments (Figure 1, Table S2).

### 252 3.3 The effects of increased CO<sub>2</sub> and the DFB addition on particulate metal concentrations

253 Increased CO<sub>2</sub> and the DFB addition did not significantly affect the concentrations of particulate Al, Ti, Cu, and Pb  
254 (Tables 1 and S2). Similarly, the addition of DFB did not directly influence particulate concentrations of Fe, but high  
255 CO<sub>2</sub> had a significant negative impact on particulate Fe (Tables 1 and S2, Figure 1). Particulate Cd concentrations were  
256 also inversely affected by CO<sub>2</sub>, but only in the presence of DFB (CO<sub>2</sub>; and CO<sub>2</sub> x DFB effect, Tables 1 and S2, Figure  
257 1). All other elements (P, Co, Zn, Mn and Mo) exhibited significant effects by CO<sub>2</sub> and by DFB, but there was also a  
258 significant interaction between these two factors (Table 1, S2). This indicates that, for example, particulate Mn, Zn, Mo,

259 Co, and P concentrations were significantly decreased by high CO<sub>2</sub>, but only in the +DFB treatments (Figure 1, Table 1,  
260 S2.). Similarly, the addition of DFB significantly increased pZn and pMn, but only at ambient CO<sub>2</sub> levels (Figure 1,  
261 Tables 1, S2).

### 263 3.4 Phosphorous-normalized metal ratios in particles collected from the mesocosms and the effects of increased 264 CO<sub>2</sub> and the DFB addition on these ratios

265 The P-normalized metal ratios (Figure 2 and means in Table 2) were highest for Al and Fe (mean: 70 ± 38 mmol Al:  
266 mol P, and 39 ± 34 mmol Fe: mol P), and lowest for Cd and Co (mean 0.02 ± 0.01 mmol Cd: mol P, and 0.07 ± 0.02  
267 mmol Co: mol P). Fe:P and Ti:P were not significantly affected by increased CO<sub>2</sub> and/or the DFB addition, but showed  
268 a significant decrease over time (Table 3). The P-normalized Cu, Co and Zn ratios changed significantly over time  
269 (Table 3). Increased CO<sub>2</sub> significantly decreased Co, Zn and Mn:P ratios, while it increased Cu:P ratios (Figure 2, Table  
270 3). DFB did not affect the Me:P ratios of any of these bioactive elements (Table 3).

## 272 4. Discussion

### 273 4.1 The effects of CO<sub>2</sub> and dFe on the plankton community

274 In this experiment we investigated changes in particulate trace metal concentrations, in response to increased CO<sub>2</sub>  
275 and/or an addition of the siderophore DFB in a coastal mesocosm experiment. For a better understanding of the  
276 processes affecting these stressors, we briefly summarise the mesocosm experiment results originating from Segovia et  
277 al. (2017). High CO<sub>2</sub>, as well as the DFB addition elevated dFe concentration increasing Fe availability (see Segovia et  
278 al. 2027 for further details). The higher dFe concentrations were sustained in the DFB treatments, suggesting that DFB  
279 significantly increased the solubility of Fe, as previously shown (Chen et al. 2004). A bloom of the coccolithophore  
280 *Emiliana huxleyi* was observed in the ambient CO<sub>2</sub> treatments, and was especially massive in the presence of DFB  
281 (LC+DFB). Our results suggest that *E. huxleyi* is able to utilise DFB-bound Fe (Fe-DFB). Indeed, *E. huxleyi* has  
282 been shown to produce a wide range of organic compounds with high affinity for Fe (Boye & Van den Berg 2000).  
283 Furthermore, *E. huxleyi* is able to acquire Fe from organic Fe complexes (Hartnett et al. 2012), including Fe-DFB  
284 (Shaked & Lis 2012, Lis et al. 2015). Indeed, the biomass of *E. huxleyi* was negatively affected by increased CO<sub>2</sub>.  
285 However, increased dFe partially mitigated the negative effect of elevated CO<sub>2</sub>, indicating that the coccolithophore was  
286 able to acclimate better to ocean acidification when Fe availability was high. High dFe also had a positive effect on the  
287 cyanobacterium *Synechococcus sp.*, while the rest of the plankton food web did not response to the treatments (Segovia  
288 et al. 2017).

Eliminado: increased

### 289 4.2 Particulate Fe and Ti are associated with lithogenic sources, while particulate Co, Cu, Zn, Cd, Mo and Mn 290 are associated with biogenic sources

291 The particulate trace metal concentrations (nM, mean of all treatments and dates) during the experiment were highest  
292 for Al, Fe and Zn, and lowest for Co and Cd, following this trend: Al ≈ Fe ≈ Zn > Ti > Cu ≈ Mn > Mo ≈ Pb > Co > Cd.  
293 Lithogenic particles are enriched in Al and low in P (average crustal Al and P content is 2.9 mmol Al and 0.034 mmol  
294 P g<sup>-1</sup> dry weight, Taylor 1964), while biogenic particles are enriched in P and low in Al (average plankton Al and P  
295 content is 0.001 mmol Al and 0.26 mmol P g<sup>-1</sup> dry weight, Bruland et al. 1991). Therefore, the distinct high abundance  
296 of Al and P in lithogenic and biogenic particles, respectively, can be used to evaluate the relative contribution of  
297 lithogenic and biogenic material in our particulate samples. In order to do this, first, it is important to establish that the  
298 vast majority of the measured particulate P is associated the biogenic fraction. In this study, the abiotic P was estimated  
299 using particulate Al concentrations (nM) and the P:Al ratio in crustal material, and was calculated to be negligible (<  
300 1% of the total measured particulate P). In addition, a significant correlation (p< 0.003) was found between particulate

Con formato: Fuente: Negrita

Eliminado: ¶

P concentrations and phytoplankton biomass (Table 4). Therefore, we assume a constant trace metal composition in biogenic particles (assuming they are rich in phytoplankton) and lithogenic particles (assuming they are rich in crustal material). We then calculated the expected metal concentrations in the particulate samples assuming that all the P measured in the particles is associated with a biogenic fraction, and that all Al in the particles is associated with the lithogenic fraction. Thus, for a given trace metal, its expected particulate trace metal concentration in seawater (mol L<sup>-1</sup>) can be calculated as the sum of the contribution from biogenic and lithogenic particles, so that:

$$[\text{Me}] = a [\text{P}] + b [\text{Al}]$$

where [Me] is the total concentration of the metal (mol L<sup>-1</sup>) expected in the particulate sample; [P] is the P concentration measured in the particles (mol L<sup>-1</sup>); [Al] is the Al concentration measured in the particles (nM L<sup>-1</sup>); *a* is the average, well-known metal content in biogenic particles, normalized to P (i.e. mol Me: mol P in marine plankton; Ho 2006) and *b* is the average, well known metal content in lithogenic particles, normalized to Al (mol Me: mol Al in the Earth crust; Taylor 1964). For example, on day 21 in the HC-DFB treatment, the concentrations of particulate Al and P were 8.22 and 134.8 nM, respectively (Table S2). Assuming a constant 0.0051 mol Fe: mol P in biogenic particles (Ho 2006) and 0.331 mol Fe: mol Al in lithogenic particles (Taylor 1964; Table 2), we calculated an expected particulate Fe concentration of 3.41 nM, where 80% was associated with lithogenic material and 20% with biogenic material. Similar calculations were made for the bioactive metals Mn, Co, Cu, Zn, Cd, and Mo (Table 2). Our calculations indicate that on average, particulate Fe was dominated by the lithogenic component (accounting for an average of 78% of the total expected particulate Fe), while for particulate Co, Cu, Zn, Cd, and Mo the biogenic fraction dominated (accounting for 94, 95, 99, 94 and 98%, respectively, of the total expected concentration; Table 2). Particulate concentrations of Mn were also dominated by the biogenic fraction (65% of the total), but the lithogenic fraction was also significant (35%). Moreover, the expected particulate Mn and Fe concentrations closely matched the particulate Mn and Fe concentration we measured (accounting for an average of ~ 71% of the measured Mn, and 115% of the measured Fe). For other metals (i.e. Cu, Mo and Zn), the expected particulate concentrations (nM) were lower than measured (23% of the measured pCu, and 8% of measured pZn; Table 2). This suggests that the particles were enriched in Cu, Mo, and Zn relative to what is expected based on natural marine plankton metal quotas (Bruland et al. 1991) and crustal ratios (Taylor 1964).

To further establish the lithogenic or biogenic source of the pMe in the particles, the particulate metal concentrations were normalized to the concentrations of particulate P and Al (Figure 2, and Table 2). These ratios were then compared with well-known molar ratios of metal to Al in the crust (Taylor 1964) and of metal to P ratios in marine plankton samples (Ho 2006) and cultures (Ho et al. 2003) (Table 2). The average Fe: Al (506 mmol Fe: mol Al) and Ti:Al ratios (119 mmol Ti: mol Al, Table 2) were relatively similar to crustal molar ratios (331 mmol Fe: mol Al and 39 mmol Ti: mol Al; Taylor 1964). Additional evidence for the significant lithogenic component in particulate Ti and Fe was gathered from Figure 3, where we plotted the molar ratios of the metals relative to P in the collected particles against the Al:P ratios measured in those same particles. The slope of these data [(Fe:P)/(Al:P) = mol Me: mol Al] is the ratio of Me:Al in the particles and can be compared to well-known Me:Al crustal ratio. Visually, if the data nicely fit the Me:Al line for crustal material, these metals are mainly associated with the lithogenic component, as evident for Fe and Ti (Figure 3). These combined results suggest that in our experiment, particulate Fe and Ti concentrations were enriched by lithogenic material. In support of this finding, we also found no significant correlation between particulate Fe and Ti concentrations (nM) and either the total plankton (phytoplankton and microzooplankton) or *E. huxleyi* biomass (µg C L<sup>-1</sup>; Table 4).

346

347

348

349

350

351

352

353

354

355

356

357

358

359

360

361

362

363

364

365

366

367

368

369

370

371

372

373

374

375

376

377

378

379

380

381

382

383

384

385

386

387

In contrast, when the P-normalized metal ratios in the particles collected from the mesocosms were plotted against the Al:P ratios in these particles, there were no correlations for the following metals Co, Cu, Zn, Cd, Mn and Mo (Figure 3), indicating that these particulate metals were not enriched in lithogenic material. Our measured metal: P ratios were comparable to plankton ratios in natural samples and in cultures (Table 2). The concentrations ( $\text{mol L}^{-1}$ ) of these metals (i.e. Cu, Co, Zn, Cd, Mn, Mo), as well as P, also showed significant correlations with the biomass ( $\mu\text{C L}^{-1}$ ) of *E. huxleyi* and that of total plankton cells ( $p < 0.05$ , Table 4), supporting a significant influence of the phytoplankton in the distribution of these particulate elements.

#### 4.3 Particulate metals with a strong biogenic component: their P-normalized ratios

The concentrations of particulate bioactive metals ( $\text{mol L}^{-1}$ ), with a significant biogenic component (i.e. excluding Fe) in the studied *E. huxleyi* bloom were ranked as:  $\text{Zn} > \text{Cu} \approx \text{Mn} > \text{Mo} > \text{Co} > \text{Cd}$  (Figure 1, Table S3), similar to those reported in indigenous phytoplankton populations:  $\text{Fe} \approx \text{Zn} > \text{Cu} \approx \text{Mn} \gg \text{Co} \approx \text{Cd}$ , (Twining and Baines, 2013). The only treatment where *E. huxleyi* did not dominate the community was the HC-DFB; in this treatment the ranking of these biogenic particulate trace metals was the same as that of LC+DFB (with the massive *E. huxleyi* bloom), but their concentrations were lower than those in LC+DFB. At the end of the experiment, the concentrations of these biogenic metals were, in general, comparable in both HC treatments, and lower than those in the LC treatments (Figure 1, Table S3). Therefore, high  $\text{CO}_2$  had a tendency to decrease particulate metal concentrations, especially on day 21. Given the strong correlation between concentrations of these particulate bioactive metals and phytoplankton biomass, the lower particulate concentrations in high  $\text{CO}_2$  were mainly due to low phytoplankton biomass.

Particulate Zn concentrations were especially high in the LC+DFB treatment (Figure 1), where the highest *E. huxleyi* biomass was observed. *Emiliania huxleyi* is well known for its high Zn cellular requirements ( $\sim 1\text{--}10$  for *E. huxleyi* vs.  $1\text{--}4$   $\text{mmol Zn: mol P}$  for other phytoplankton; Sunda and Hunstman 1995, Sunda 2013). But, the Zn: P ratios in the LC+DFB treatment (range  $45\text{--}69$   $\text{mmol Zn: mol P}$ ; Figure 2, Table S2), as well as in all the other treatment (range  $16\text{--}34$   $\text{mmol Zn: mol P}$ ; Figure 2, Table S2) were significantly higher than these published ratios. This could be explained by, the adsorption of these metals to the outside of the cells, and/or anthropogenic inputs of Zn into the fjord. The Zn:P ratios in the samples washed with the oxalate-EDTA were still high (range  $28\text{--}57$  for LC+DFB and  $16\text{--}33$   $\text{mmol Zn: mol P}$  in all other treatments, Table S3), thus adsorption might have not been significant. We hypothesize that anthropogenic aerosols which are rich in anthropogenic particulate metals, such as Zn and Cu (Perry et al. 1999; Narita et al. 1999), and have high percentage of Zn and Cu dissolution (ref.), might be the source of these high Zn concentrations and ratios in the particles.

Similarly, the Cu:P ratios in the collected particles were relatively elevated ( $1.4 \pm 0.8$   $\text{mmol Cu: mol P}$ ) compared to those of other phytoplankton, including *E. huxleyi* (Table 2). The dissolved ( $7.7 \pm 0.41$   $\text{nM Cu}$ , Figure S3) and particulate Cu concentrations ( $0.35 \pm 0.25$   $\text{nM}$ , Table S2) in our experiment were high, and similar to those previously measured in this fjord (Muller et al., 2005). Rain events (or wet deposition of anthropogenic aerosols) in this fjord result in high dissolved Cu and the active production of strong organic ligands by *Synechococcus*—to lower the free Cu concentrations (Muller et al., 2005). Therefore, high Cu might be a general condition in this fjord due to the rainy nature of the geographical location, and indigenous plankton might have developed physiological mechanisms to deal with high Cu, such as the production of organic ligands to prevent uptake (Vraspir and Butler, 2009), or of heavy-metal-binding peptides (phytochelatins) to lower Cu toxicity inside the cell (Ahner and Morel, 1995; Ahner et al., 1995;

Eliminado: 4

389 Knauer et al., 1998). Since we measured high particulate Cu, and Cu:P in our experiment, *E. huxleyi* might have been  
390 relying mainly on phytochelatins to buffer high intracellular Cu (Ahner et al., 2002).

391  
392 The Cd:P ratios (average  $0.024 \pm 0.01$  mmol Cd:mol P, Figure 2) were significantly lower than those in phytoplankton  
393 and *E. huxleyi* (0.36 mmol Cd:mol P, Figure 2). This was surprising, because Cd quotas are normally higher in  
394 coccolithophores than in diatoms and chlorophytes (Sunda and Huntsman, 2000; Ho et al., 2003). High Cd quotas in  
395 coccolithophores have been suggested to result from accidental uptake through Ca transporters and channels (Ho et al.,  
396 2009). The low Cd quotas here may be explained by the antagonistic interaction between Mn and Cd or Zn and Cd  
397 under high Mn and Zn, respectively (Sunda and Huntsman, 1998, 2000; Cullen and Sherrell, 2005).  
398 Since high Zn:P ratios were common in this study ( $34.02 \pm 18.05$  mmol Zn:mol P, Figure 2), we hypothesize that high  
399 Zn levels antagonistically interacted with Cd, resulting in low Cd:P ratios in the particles.

#### 400 401 **4.4 The effects of increased CO<sub>2</sub> and the DFB addition on particulate metal concentrations and P-normalized** 402 **ratios**

403 Fe enrichment is common in coastal waters, due to sediment resuspension, rivers input, aeolian deposition and mixing  
404 or upwelling of deep water. Indeed, Fe was the essential metal with the highest particulate concentrations in our study  
405 (Figure 1, Table 3). Furthermore, in this study particulate Fe was characterized by a strong lithogenic component, and  
406 was not correlated with phytoplankton biomass. Fe was also unique, in that it was the only trace element whose  
407 particulate concentration was significantly and exclusively affected by CO<sub>2</sub> (no interaction between CO<sub>2</sub> and  
408 DFB), regardless of the presence or absence of DFB (Table 1). Furthermore, particulate Fe concentrations (nM)  
409 decreased steadily between days 12 and 21, with the exception of the control treatment (LC-DFB; Figure 1, Table 2S).  
410 This suggests that the increase in CO<sub>2</sub> and/or the DFB addition reduce the concentration of pFe, despite the  
411 phytoplankton bloom. Such a decrease in pFe (range 2.3-fold in LC-DFB, vs. 13.7-fold in HC+DFB; Table S2) might  
412 be mediated by the dissolution of particulate Fe by low pH or by the presence of strong organic chelators as observed in  
413 this very experiment (Segovia et al. 2017 and references therein) where dFe notably increased in treatments with high  
414 CO<sub>2</sub> and/or the addition of DFB (Figure S3). Furthermore, the dissolution of particulate Fe in the treatments with high  
415 CO<sub>2</sub> and/or the addition of DFB was evident in the Fe partitioning coefficients—the molar ratio between particulate and  
416 dissolved concentrations (Figure 4). On day 21, the Fe partitioning coefficients varied by 22-fold between the highest  
417 for the control (LC-DFB: 1.039) and lowest for the HC+DFB treatments (HC+DFB: 0.047; Figure 4). Thus, either the  
418 DFB addition or high CO<sub>2</sub> promoted the dissolution of pFe. However, at the end of the experiment, high dFe  
419 concentrations were only observed in the treatments with the DFB additions, suggesting that the presence of strong  
420 organic Fe chelators, such as DFB, mediated the maintenance of high dissolved Fe concentrations, as previously  
421 observed (Segovia et al. 2017). Thus, in our future oceans, high CO<sub>2</sub> (low pH) will increase dissolved Fe concentrations  
422 in regions rich in particulate Fe, and in strong organic Fe chelators. The deleterious effects of OA on the development  
423 of ecologically important species sensitive to increased CO<sub>2</sub> such as *E. Huxleyi*, will be more relevant in high-Fe  
424 environments than in Fe-limited ones.

425 In contrast to the findings for Fe, particulate Cu concentrations a) were not affected by either high CO<sub>2</sub> or the DFB  
426 addition; b) were dominated by a biogenic component and c) were significantly correlated with phytoplankton biomass  
427 (Table 4). Furthermore, unique to Cu was a significant increase in Cu:P ratios by day 21 in the high CO<sub>2</sub> treatments,  
428 especially when no DFB was added. Since the Cu partitioning coefficients only varied by 3.25 fold among treatments  
429 on day 21 (LC-DFB: 0.065 vs. HC+DFB: 0.047; data not shown), we hypothesize that high CO<sub>2</sub> did not affect the  
430 partitioning between particulate and dissolved Cu, but instead, it affected the speciation of dissolved Cu, increasing free

431 Cu ( $\text{Cu}^{2+}$ ) and thus, its bioavailability. This resulted in the highest Cu:P ratios in the high  $\text{CO}_2$  treatments, despite the  
432 low phytoplankton biomass. This increase in bioavailability under lower pH is typical of metals that form strong  
433 inorganic complexes with carbonates, such as  $\text{Cu}^{2+}$  (Millero et al., 2009). Thus in our future oceans, high  $\text{CO}_2$  (low pH)  
434 will shift the speciation of dissolved Cu towards higher abundance of free ionic species, increasing its bioavailability  
435 and likely its toxicity.

436  
437 Similarly to Cu, particulate Co, Zn and Mn were correlated with biomass and were dominated by the biogenic  
438 component. But in contrast to Cu, these metals particulate concentrations were affected by increased  $\text{CO}_2$  and/or the DFB  
439 addition. However, the effects of high  $\text{CO}_2$  and/or DFB were very complex because significant interactions between  
440 these 2 factors were observed (Table 1); and further studies are required before we are able to discern and conclude a  
441 significant trend. Yet, the P-normalized ratios of Co, Zn and Mn were significantly affected by  $\text{CO}_2$  (Table 3),  
442 exhibiting moderately lower ratios under high  $\text{CO}_2$ , when phytoplankton biomass was lowest. These results imply that  
443 the bioavailability of these metals was not enhanced under acidic conditions. This suggests that under high  $\text{CO}_2$  (low  
444 pH) the free ionic species of these metals will not significantly increase in the future, as shown for metals that occur  
445 predominantly as free ionic species in seawater (Millero et al., 2009).

## 446 5. Concluding remarks

447 The results presented here show that in the fjord where we carried out the present experiment, particulate Fe was  
448 dominated by lithogenic material, and was significantly decreased in the treatments with high  $\text{CO}_2$  concentrations  
449 and/or the DFB addition. Indeed, high  $\text{CO}_2$  and/or DFB promoted the dissolution of particulate Fe, and the presence  
450 of this strong organic complex helped maintaining high dissolved Fe. This shift between particulate and dissolved  
451 Fe, in the presence of DFB, promoted a massive bloom of *E. huxleyi* in the treatments with ambient  $\text{CO}_2$ , due to  
452 increased dissolved Fe. During the bloom of *E. huxleyi*, the concentrations of particulate metals ( $\text{mol L}^{-1}$ ) with  
453 a strong biogenic component (Cu, Co, Zn, Cd, Mn, and Mo) were a) highly dynamic, b) positively correlated with  
454 plankton biomass, and c) influenced by growth requirements. Furthermore, high  $\text{CO}_2$  decreased the Me:P ratios of Co,  
455 Zn and Mn, while increased the Cu:P ratios. In contrast DFB had no effects on these ratios. According to our results,  
456 high  $\text{CO}_2$  may decrease particulate Fe and increase dissolved Fe, but high concentrations of dissolved Fe will only be  
457 maintained by the presence of strong organic ligands. Furthermore, ocean acidification will decrease *E. huxleyi*  
458 abundance, and as a result, the sinking of particulate metals enriched in *E. huxleyi*. Moreover, the Me:P ratios of metals  
459 that are predominately present in an ionic free form in seawater (e.g. Co, Zn and Mn) will likely decrease or stay  
460 constant. In contrast, high  $\text{CO}_2$  is predicated to shift the speciation of dissolved metals associated with carbonates, such  
461 as Cu, increasing their bioavailability, and resulting in higher Me:P ratios. We suggest that high Cu might be a  
462 common condition in this fjord, and autochthonous plankton might be able to cope with high Cu levels by developing  
463 specific physiological mechanisms. Future high  $\text{CO}_2$  levels are expected to change the relative concentrations of  
464 particulate and dissolved metals, due to the differential effects of high  $\text{CO}_2$  on trace metal solubility, speciation,  
465 adsorption and toxicity, as well as on the growth of different phytoplankton taxa, and their elemental trace metal  
466 composition.

## 467 Acknowledgments

468  
469 This work was funded by CTM/MAR 2010-17216 (PHYTOSTRESS) research grant from the Spanish Ministry for  
470 Science and Innovation (Spain) to MS, and by NSERC grants (Canada) to MTM and JTC. MRL was funded by a FPU  
471 grant from the Ministry for Education (Spain) and by fellowships associated to the mentioned above research grants to  
472 carry out a short-stay at MTM and JTC laboratories to analyze dissolved and particulate metals. We thank all the  
473

**Eliminado:** The decrease in particulate Fe may affect the sinking flux of other metals associated with Fe oxides in open ocean settings. Furthermore, ocean acidification will decrease

478 participants of the PHYTOSTRESS experiment for their collaboration, and the MBS (Espesrend, Norway) staff for  
 479 logistic support during the experiment. We thank the anonymous reviewers for insightful comments and constructive  
 480 criticisms.

Eliminado: two

Eliminado: very

# 481 **Conflict of interest**

482 Authors declare no conflict of interest.

Con formato: Fuente: Sin Negrita

Con formato: Fuente: Sin Negrita

# 484 **References**

485 Ahner, B.A., Liping, W., Oleson, J.R., Ogura, N.: Glutathione and other low molecular weight tiols in marine  
 486 phytoplankton under metal stress, Mar. Ecol. Prog. Ser., 232, 93-103, 2002.  
 487 Behrenfeld, M.J., Milligan, A.J.: Photophysiological expressions of iron stress in phytoplankton, Ann. Rev. Mar. Sci.  
 488 5, 217–246, 2013.

489 Boye M, van den Berg CMG (2000) Iron availability and the release of iron-complexing ligands by *Emiliania huxleyi*.  
 490 Mar Chem 70:277–287

Con formato: Inglés (americano)

491 Canadell, J.G., Quéré, C., Raupach, M.R., Field, C.B., Buitenhuis, E.T., Ciais, P., Conway, T.J., Gillet, N.P.,  
 492 Houghton, R.A., Marland, G.: Contributions to accelerating atmospheric CO<sub>2</sub> growth from economic activity, carbon  
 493 intensity, and efficiency of natural sinks. Proc. Natl. Acad. Sci. USA 104, 18886-18870, 2007

494 Chen, M., W.-X. Wang, and L. Guo (2004). Phase partitioning and solubility of iron in natural seawater controlled by  
 495 dissolved organic matter, Global Biogeochem. Cycles, 18, GB4013, doi:10.1029/2003GB002160.

Con formato: Inglés (americano)

496 Crawford, D.W., Lipsen, M.S., Purdie, D.A., Lohan, M.C., Statham, P.J., Whitney, F.A., Putland, J.N., Johnson, W.K.,  
 497 Sutherland, N., Peterson, T.D., Harrison, P.J., Wong, C.S.: Influence of zinc and iron enrichments on phytoplankton  
 498 growth in the northeastern subarctic Pacific. Limnol. Oceanogr., 48,1583–1600, 2003.

Con formato: Fuente: 12 pto, Color de fuente: Negro, Español

499 Cullen, J.T., Sherrell, R.M.: Effects of dissolved carbon dioxide, zinc, and manganese on the cadmium to phosphorus  
 500 ratio in natural phytoplankton assemblages, Limnol. Oceanogr. 50, 1193–1204, 2005.

Con formato: Sangría: Izquierda: 0 cm, Primera línea: 0 cm, Control de líneas viudas y huérfanas

501 Desboeufs, K.V. A. Sofikitis, R. Losno, J.L. Colin, P. Ausset. 2005. Dissolution and solubility of trace metals from  
 502 natural and anthropogenic aerosol particulate matter Chemosphere 58 (2): 195-203 DOI:  
 503 10.1016/j.chemosphere.2004.02.025

504 Dymond, J., Lyle, M.: Flux comparisons between sediments and sediment traps in the eastern tropical Pacific:  
 505 implications for atmospheric CO<sub>2</sub> variations during the Pleistocene. Limnol. Oceanogr, 30, 699–712, 1985

506 Field, C.B.: Primary production of the biosphere: Integrating terrestrial and oceanic components, Science 281, 237–240,  
 507 1998.

508 Frew, R.D., Hutchins, D.A., Nodder, S., Sanudo-Wilhelmy, S., Tovar-Sanchez, A., Leblanc, K., Hare, C.E., Boyd,  
 509 P.W.: Particulate iron dynamics during Fe Cycle in subantarctic waters southeast of New Zealand, Glob. Biogeochem.  
 510 Cycles 20, GB1S93. [http://dx. doi.org/10.1029/2005GB002558](http://dx.doi.org/10.1029/2005GB002558), 2006.

511 Guo, J., Lapi, S., Ruth, T.J., Maldonado, M.T.: The effects of iron and copper availability on the copper stoichiometry  
 512 of marine phytoplankton. J. Phycol, 48, 312–325, 2012.

513 Hartnett, A., Böttger, L.H., Matzanke, B.F., Carrano, C.J (2012) Iron transport and storage in the coccolithophore:  
 514 *Emiliania huxleyi*. Metallomics 4:1127-1227

515 Ho, T-Y.: The trace metal composition of marine microalgae in cultures and natural assemblages. In: Rao S (ed) Algal  
 516 cultures, analogues of blooms and applications, Science Publishers, New Hampshire, p 271–299, 2006.

Eliminado: ¶

517 Ho, T., Quigg, A., Zoe, V., Milligan, A.J., Falkowski, P.G., Morel, M.M.: The elemental composition of some marine  
 518 phytoplankton. J. Appl. Phycol 1159,1145–1159, 2003

519 Ho, T-Y., Wen, L-S., You, C-F., Lee, D-C.: The trace metal composition of size-fractionated plankton in the South  
 520 China Sea: Biotic versus abiotic sources. Limnol. Oceanogr, 52, 1776–1788, 2007.

521 Ho, T-Y., You, C.F., Chou, W-C., Pai, S-C., Wen, L-S., Sheu, D.D.: Cadmium and phosphorus cycling in the water  
 522 column of the South China Sea: The roles of biotic and abiotic particles, Mar. Chem. 115-125-133, 2009.

523 Hoffmann, L.J., Breitbarth, E., Boyd P.W., Hunter, K.A.: Influence of ocean warming and acidification on trace metal  
 524 biogeochemistry, Mar Ecol Prog Ser 470-191–205, 2012.

525 Hutchins, D., Mulholland, M., Fu, F.: Nutrient cycles and marine microbes in a CO<sub>2</sub>-enriched ocean, Oceanography  
 526 22-128–145, 2009.

527 Hutchins DA (2011) Forecasting the rain ratio. Nature 476: 41–42

528 Jakuba, R.W., Moffett, J.W., Dyhrman, S.T.: Evidence for the linked biogeochemical cycling of zinc, cobalt, and  
 529 phosphorus in the western North Atlantic Ocean, Global Biogeochem. Cycles 22, GB4012, 2008.

530 Johnson et al. 2007. Developing Standards for Dissolved Iron in Seawater. EOS Transactions American Geophysical  
 531 Union 88 (11): p. 131-132

Con formato: Fuente: 10 pto, Inglés (americano)

Con formato: Sangría: Izquierda: 0 cm, Sangría francesa: 0.25 cm

532 King, A.L., Sanudo-Wilhelmy, S.A., Boyd, P.W., Twining, B.S., Wilhelm, S.W., Breene, C., Ellwood, M.J. and  
 533 Hutchins, D.A.: A comparison of biogenic iron quotas during a diatom spring bloom using multiple approaches,  
 534 Biogeochemistry 9, 667–687, 2012.



540 Kuma K, Nishioka J, Matsunaga K. Controls on iron(III) hydroxide solubility in seawater: the influence of pH and  
541 natural organic chelators. *Limnol Oceanogr* 41:396–407.1996.

542 [Lis H, Shaked Y, Kranzler C, Keren N, Morel FMM \(2015\) Iron bioavailability to phytoplankton: an empirical](#)  
543 [approach. \*Isme J\* 9:1003–1013](#)

544 Lorenzo MRL, Iñiguez C, Egge J, Larsen A, Berger SAB, Garcia-Gomez C, Segovia M. Increased CO<sub>2</sub> and iron  
545 availability effects on carbon assimilation and calcification on the formation of *Emiliania huxleyi* blooms in a coastal  
546 phytoplankton community. *Env. Exp. Bot.* 148:47-58, 2018.

547 Mackey, K.R.M., Morris, J.J., Morel, F.M.M.: Response of photosynthesis to ocean acidification, *Oceanography* 28,74–  
548 91, 2015.

549 Marchetti A, Maldonado MT. Iron. In: Borowitzka MA, Beardall J, Raven JA (eds) *The physiology of microalgae*.  
550 Springer International Publishing, Cham., p 233–279.2016.

551

552 Millero, FJ, Sotolongo, S & Izaguirre, M. The oxidation kinetics of Fe(II) in seawater. *Geochim. Cosmochim. Acta*,51,  
553 793–801. 1987.

554

555 Millero, F.J., Woosley, R., Ditrolio, B., Waters, J.: Effect of ocean acidification on the speciation of metals in seawater,  
556 *Oceanography* 22:72–85, 2009.

557 Morel, F.M., Price, N.M.: The biogeochemical cycles of trace metals in the oceans, *Science* 300, 944–947, 2003.

558 Muller, F.L., Larsen, A., Stedmon, C.A., Søndergaard, M.: Interactions between algal – bacterial populations and trace  
559 metals in fjord surface waters during a nutrient-stimulated summer bloom, *Limnol Oceanogr* 50, 1855–1871, 2005.

560 Öztürk M, Steinnes E, Sakshaug E. Iron speciation in the Trondheim Fjord from the perspective of iron limita- tion for  
561 phytoplankton. *Estuar Coast Shelf Sci* 55:197–212. 2002.

562 Paasche, E.: A review of the coccolithophorid *Emiliania huxleyi* (Pymnesiophyceae), with particular reference to  
563 growth, coccolith formation, and calcification-photosynthesis interactions, *Phycologia* 40, 503–529, 2002.

564 Price, N.M., Morel, F.M.M.: Cadmium and cobalt substitution for zinc in a marine diatom, *Nature* 344, 658–660, 1990.

565 Rauschenberg, S., Twining, B.S.: Evaluation of approaches to estimate biogenic particulate trace metals in the ocean,  
566 *Mar Chem* 171, 67–77, 2015

567 Riebesell, U., Tortell, P.D.: Effects of ocean acidification on pelagic organisms and ecosystems, In: Gattuso J-P,  
568 Lansson L (eds) *Ocean Acidification*. Oxford University Press., Oxford, p 99–121, 2011.

569 Robbins, L.L., Hansen, M.E., Kleypas, J.A., Meylan, S.C.: CO<sub>2</sub>calc: A User Friendly Carbon Calculator foe Windows,  
570 Mac OS X and iOS (iPhone), Open File Rep. 2010-1280, 2010.

571 Sanudo-Wilhelmy, S.A., Tovar-Sanchez, A., Fu, F.X., Capone, D.G., Carpenter, E.J., Hutchins, D.A.: The impact of  
572 surface-adsorbed phosphorus on phytoplankton Redfield stoichiometry, *Nature* 432, 897–901, 2004.

573 Semeniuk, D.M, Bundy, R.M., Posacka, A.M., Robert, M., Barbeau K.A., Maldonado, M.T.: Using <sup>67</sup>Cu to study the  
574 biogeochemical cycling of copper in the northeast subarctic Pacific ocean, *Frontiers Mar. Sci.* 3, 2-19, 2016.

575 [Shaked Y, Lis H \(2012\) Disassembling iron availability to phytoplankton. \*Front Microbiol\* 3:123](#)

576 Segovia, M., Lorenzo, M.R., Maldonado, M.T., Larsen, A., Berger, S.A., Tsagaraki, T.M., Lázaro, F.J., Iñiguez, C.,  
577 García-Gómez, C., Palma, A., Mausz, M.A., Gordillo, F.J.L., Fernández, J.A., Ray, J. L., Egge, J.K.: iron availability  
578 modulates the effects of future CO<sub>2</sub> levels within the marine planktonic food web, *Mar. Ecol. Progr. Ser.* 565, 17–33,  
579 2017.

580 Segovia M, M Rosario Lorenzo, Concepción Iñiguez, Candela García-Gómez. Physiological stress response associated  
581 with elevated CO<sub>2</sub> and dissolved iron in a phytoplankton community dominated by the coccolithophore *Emiliania*  
582 *huxleyi* Marine. *Ecol.Progr. Ser.* 586: 73–89.2018.

583 Shi, D., Xu, Y., Hopkinson, B.M., Morel, F.M.M.: Effect of ocean acidification on iron availability to marine  
584 phytoplankton, *Science* 327, 676–679, 2010.

585 Stocker, T.F., Qin, D., Plattner, G-K., Tignor, M., Allen, S.K., Boschung, J., Nauels, A., Xia, Y., Bex, V., Midgley,  
586 P.M. (Eds) *IPCC, 2013: Climate Change 2013: The Physical Science Basis. Contribution of Working Group I to the*  
587 *Fifth Assessment Report of the Intergovern- mental Panel on Climate Change*. Cambridge University Press,  
588 Cambridge, United Kingdom and New York, NY, USA, 2013.

589 Sunda, W.G., Huntsman, S.A.: iron uptake and growth limitation in oceanic and coastal phytoplankton, *Mar. Chem.* 50,  
590 189–206, 1995a.

591 Sunda, W.G., Huntsman, S.A.: Cobalt and zinc interreplacement in marine phytoplankton: biological and geochemical  
592 implications, *Limnol. Oceanogr.* 40, 1404–1417, 1995b.

593 Sunda, W.G., Huntsman, S.A. Control of Cd concentrations in a coastal diatom by interactions among free ionic Cd,  
594 Zn, and Mn in seawater, *Environ Sci Technol* 32:2961–2968, 1998.

595 Sunda, W.G., Huntsman, S.A.: Effect of Zn, Mn, and Fe on Cd accumulation in phytoplankton: implications for oceanic  
596 Cd cycling, *Limnol. Oceanogr.* 45, 1501–1516, 2000.

597 Sunda, W.G.: Feedback interactions between trace metal nutrients and phytoplankton in the ocean, *Front Microbiol* 3,

Con formato: Normal (Web), Sangría: Izquierda: 0 cm, Sangría francesa: 0.25 cm, Interlineado: sencillo, Control de líneas viudas y huérfanas, Ajustar espacio entre texto latino y asiático, Ajustar espacio entre texto asiático y números

Con formato: Fuente: Times New Roman, 10 pto

Con formato: Fuente: Times New Roman, 10 pto, Color de fuente: Color personalizado(RGB(25;25;30))

Eliminado: ¶

Con formato: Español

Con formato: Español

599 204, 2012.  
 600 Tang, D.G., Morel, F.M.M.: Distinguishing between cellular and Fe-oxide-associated trace elements in phytoplankton,  
 601 Mar. Chem. 98, 18–30, 2006.  
 602 Taylor, S.: Abundance of chemical elements in the continental crust: a new table. Geochim Cosmochim Acta 28, 1273–  
 603 1285, 1964.  
 604 Tovar-Sanchez, A., Sanudo-Wilhelmy, S.A., Garcia-Vargas, M., Weaver, R.S., Popels, L.C., Hutchins, D.A.: A trace  
 605 metal clean reagent to remove surface-bound iron from marine phytoplankton, Mar. Chem. 82, 91–99, 2003.  
 606 Tovar-Sanchez, A., Sanudo-Wilhelmy, S.A., Kustka, A.B., Agustí, S., Dachs, J., Hutchins, D.A., Capone, D.G. and  
 607 Duarte, C.M.: Effects of dust deposition and river discharges on trace metal composition of *Trichodesmium* spp. in  
 608 the tropical and subtropical North Atlantic Ocean, Limnol Oceanogr 51, 1755–61, 2006.  
 609 Twining, B.S., Baines, S.B.: The trace metal composition of marine phytoplankton, Ann Rev Mar Sci 5, 191–215,  
 610 2013.  
 611 Xu, Y., Tang, D., Shaked, Y., Morel, F.M.M.: Zinc, cadmium, and cobalt interreplacement and relative use efficiencies  
 612 in the coccolithophore *Emiliania huxleyi*, Limnol Oceanogr 52, 2294–2305, 2007.  
 613 Zamzow, H., Coale, K.H., Johnson, K.S., Sakamoto, C.M.: Determination of copper complexation in seawater using  
 614 flow injection analysis with chemiluminescence detection, Anal Chim Acta 377, 133–144, 1998.  
 615 Zondervan, I.: The effects of light, macronutrients, trace metals and CO<sub>2</sub> on the production of calcium carbonate and  
 616 organic carbon in coccolithophores—A review, Deep Sea Res Part II Top Stud Oceanogr 54, 521–537, 2007.

**Table 1.** Statistical analyses (Split-plot ANOVA) of the effects of high CO<sub>2</sub>, the addition of DFB, and their interaction, as well as the effect of time, on the concentrations of particulate metals (mmol L<sup>-1</sup>, data in Table S2, and Figure 3) in particles collected from the different mesocosms treatments. We used all the days for the analyses because the Split-Plot ANOVA integrates fixed factors (Co<sub>2</sub> and Fe) and a repeated measures factor (time) by using the post-hoc Bonferroni, thus, time was fully considered during the whole experimental period.

Factor	Al	Ti	P	Fe	Cu	Co	Zn	Cd	Mn	Mo	Pb
CO <sub>2</sub>	ns	ns	**	*	ns	**	***	***	**	***	ns
DFB	ns	ns	*	ns	ns	*	**	ns	*	*	ns
CO <sub>2</sub> x DFB	ns	*	**	ns	ns	*	**	*	**	**	ns
Time	ns	ns	ns	***	*	***	***	***	***	***	**

*ns*: not significant; \*  $p < 0.05$ ; \*\*  $p < 0.01$ ; \*\*\*  $p < 0.001$

**Table 2.** The average metal ratios in the particles collected in this study (without oxalate wash) using the data reported in Table S2. The P-normalized ratios (mmol : mol P, Figure 4) are compared to previous estimates in marine plankton samples and phytoplankton cultures (A). The Al-normalized ratios (mmol : mol Al) are compared to crustal ratios (B).

A)

(mmol : mol P)	Mn:P	Fe:P	Co:P	Cu:P	Zn:P	Cd:P	Mo:P	Al:P	Reference
Phytoplankton <sub>Lab</sub>	3.8	7.5	0.19	0.38	0.8	0.21	0.03		Ho et al. 2003
Marine Plankton <sub>Field</sub>	0.68±0.54	5.1±1.6	0.15±0.06	0.41±0.16	2.1±0.88				Ho 2006
<i>E. huxleyi</i> <sub>Lab</sub>	7.1±0.36	3.5±0.07	0.29±0.02	0.07±0.013	0.38±0.002	0.36±0.01	0.022±0.0003		Ho et al. 2003
<b>This study</b>	1.65±0.41	39.2±34.3	0.07±0.02	1.41±0.55	34.02±18.05	0.02±0.01	0.42±0.12	70±38	
Crust ratio	510	29,738	13	25	32	0.05	0.46	89,972	Taylor 1964

B)

(mmol : mol Al)	Mn:Al	Fe:Al	Co:Al	Cu:Al	Zn:Al	Cd:Al	Mo:Al	Pb:Al	Ti:Al
Crustal ratio	5.7	331	0.14	0.27	0.35	0.001	0.005	0.02	39
<b>This study</b>	35±28	506±342	1.5±1.2	26.5±15	795±865	0.5±0.4	8.6±6.5	4.9±3.9	119±47.6

**Table 3.** Statistical analyses (Split-plot ANOVA) of the effects of CO<sub>2</sub>, DFB, and their interaction, as well as the effect of time, on the P-normalized metal quotas (mmol: mol P, data in Figure 4, and Table S2) in particles collected from the different mesocosm treatments.

Factor	Fe:P	Cu:P	Co:P	Zn:P	Cd:P	Mn:P	Mo:P	Pb:P	Ti:P
CO <sub>2</sub>	ns	*	***	**	ns	*	ns	ns	ns
DFB	ns	ns	ns	ns	ns	ns	ns	ns	ns
CO <sub>2</sub> x DFB	ns	ns	ns	ns	ns	ns	ns	ns	ns
Time	***	***	***	***	ns	ns	ns	ns	***

*ns: not significant; \*  $p < 0.05$ ; \*\*  $p < 0.01$ ; \*\*\*  $p < 0.001$*

**Table 4.** The relationship (Pearson correlations,  $p < 0.05$ ) between particulate metals concentrations (nmol L<sup>-1</sup>, no oxalate wash, reported in Table S2) and the biomass (µgC L<sup>-1</sup>) of *Emiliania huxleyi* and total cells (phytoplankton and microzooplankton) collected from the different mesocosm treatments.

		P	Fe	Cu	Co	Zn	Cd	Mn	Mo	Pb	Ti
<i>E. huxleyi</i>	Correlation coefficient	0.622	ns	0.614	0.756	0.747	0.818	0.686	0.825	ns	ns
	P-value	0.003		0.003	$7.35 \cdot 10^{-5}$	$1.01 \cdot 10^{-4}$	$6.02 \cdot 10^{-6}$	$5.93 \cdot 10^{-4}$	$4.20 \cdot 10^{-6}$		
Total cells	Correlation coefficient	0.641	ns	0.51	0.644	0.889	0.802	0.598	0.53	ns	ns
	P-value	0.002		0.02	$1.62 \cdot 10^{-3}$	$7.03 \cdot 10^{-8}$	$1.23 \cdot 10^{-5}$	$4.18 \cdot 10^{-3}$	$1.35 \cdot 10^{-2}$		

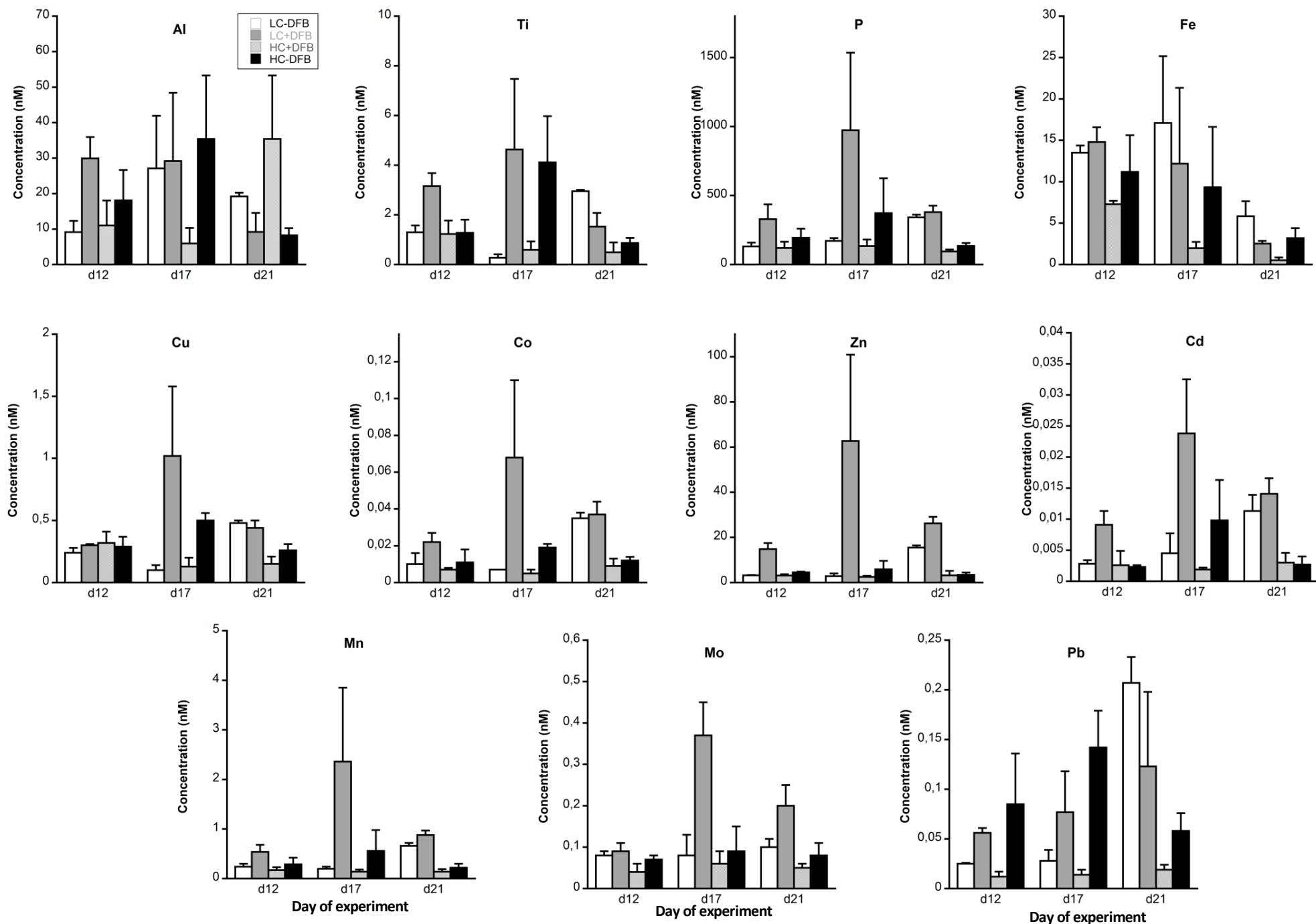


**Fig. 1.** The concentration of particulate metals in seawater (nM) in the different treatments; LC: ambient CO<sub>2</sub> (390  $\mu$ atm); HC: increased CO<sub>2</sub> (900  $\mu$ atm); -DFB (ambient dFe); +DFB (increased dFe) during the development of a bloom of *Emiliania huxleyi*. Bars are means of measurements in 3 independent mesocosms (n = 3) except for LC–DFB where n = 2. Error bars indicate SD.

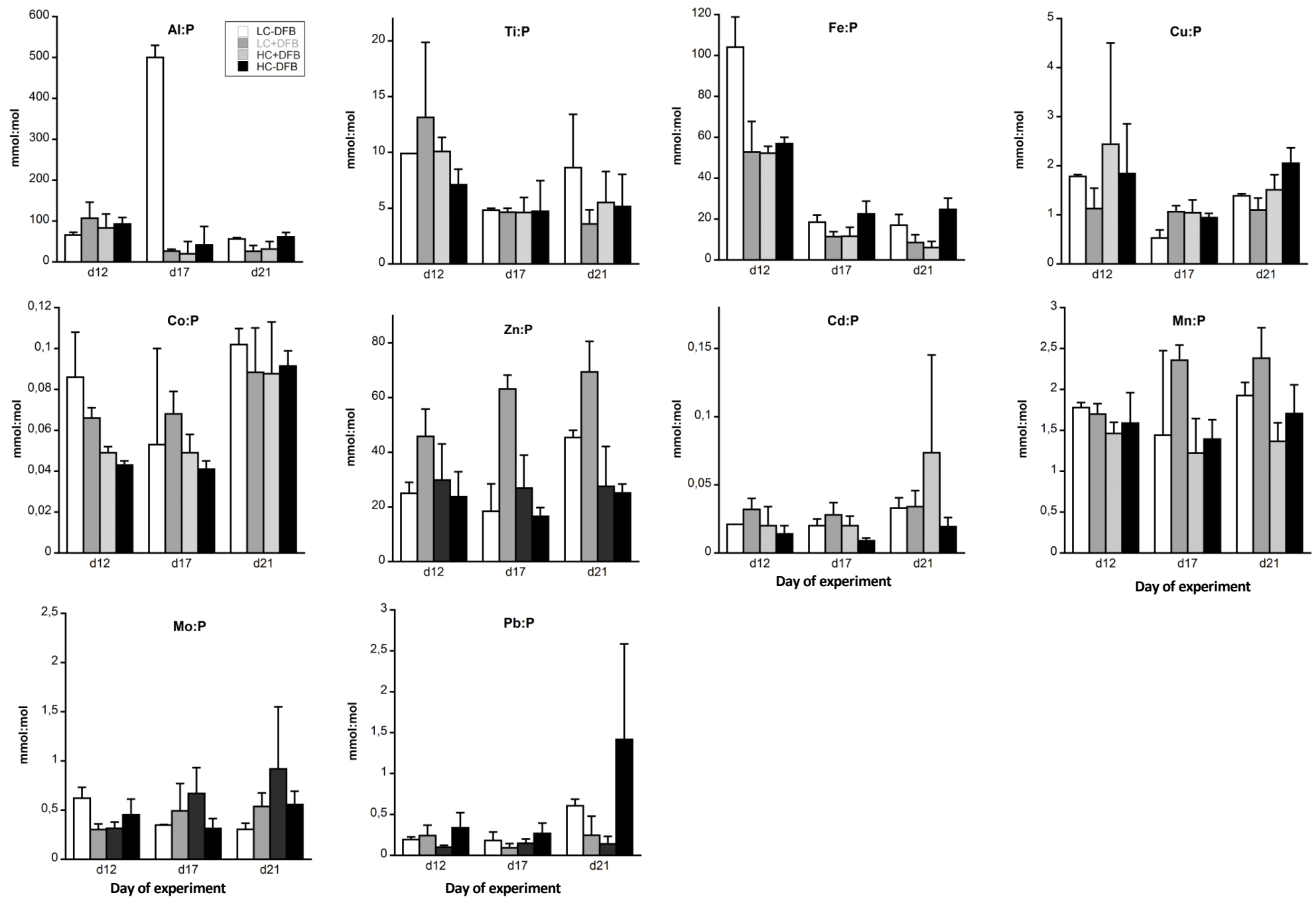


**Fig. 2.** P-normalized metal quotas (mmol:mol P) of particles from different treatments; LC: ambient CO<sub>2</sub> (390  $\mu$ atm); HC: increased CO<sub>2</sub> (900  $\mu$ atm); -DFB (ambient dFe); +DFB (increased dFe) during the development of a bloom of *Emiliana huxleyi*. Bars are means of measurements in 3 independent mesocosms (n = 3) except for LC-DFB where n = 2. Error bars indicate SD.



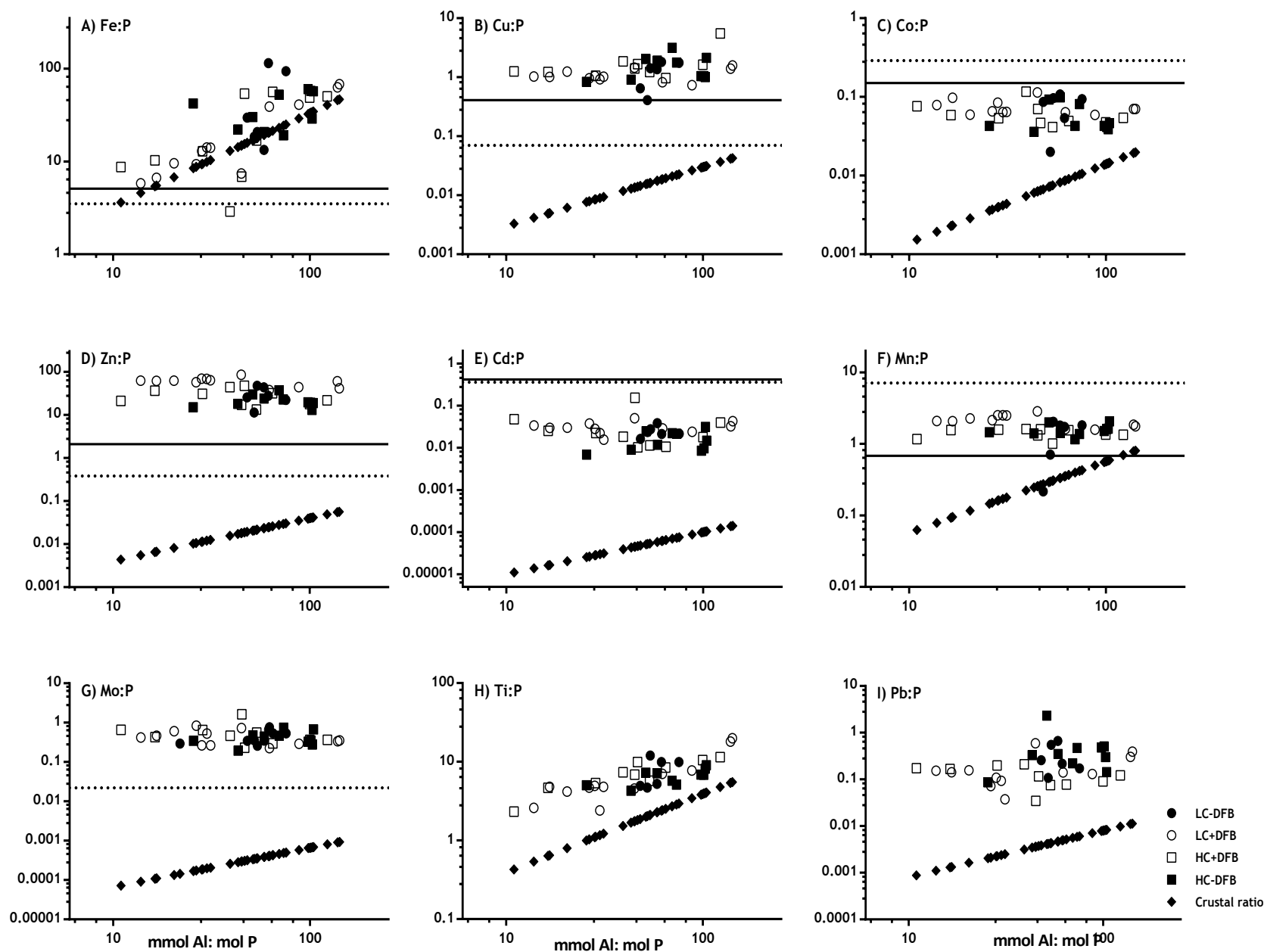


**Fig. 3.** Comparison of P-normalized metal ratios in particles (mmol:mol P) against mmol Al:mol P ratios in the same particles (without oxalate wash) collected from the different mesocosm treatments (LC: ambient CO<sub>2</sub>; HC: increased CO<sub>2</sub> (900  $\mu$ atm); -DFB: no DFB addition; +DFB: with a 70 nM DFB addition) during the development of a bloom on day 12, 17 and 21 (original data reported in Table S2). The x-axis parallel solid and dotted lines represent the average metal quotas obtained from marine plankton assemblages (Ho 2006) and from cultures of *Emiliania huxleyi* (Ho et al. 2003). The slope of the line with the  $\blacklozenge$  symbols indicates the average metal : Al (mol:mol) in crustal material (Taylor, 1964). (A) Fe:P, (B) Cu:P, (C) Co:P, (D) Zn:P, (E) Cd:P, (F) Mn:P, (G) Mo:P, (H) Ti:P, (I) Pb:P.

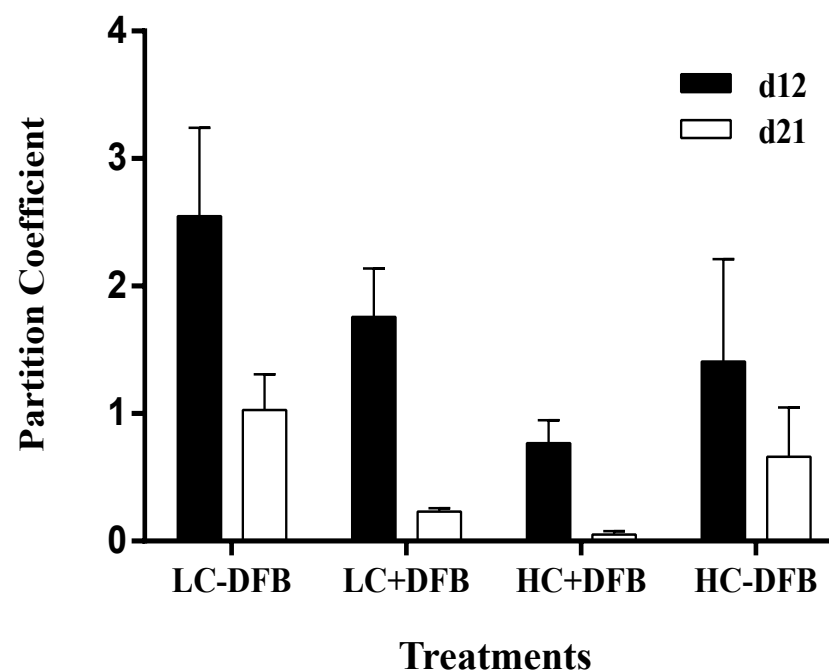


**Fig. 4.** The Fe partition coefficients (the molar ratio between particulate and dissolved concentrations) in the different mesocosm treatments; LC: ambient CO<sub>2</sub> (390  $\mu$ atm); HC: increased CO<sub>2</sub> (900  $\mu$ atm); -DFB: no DFB addition; +DFB: with a 70 nM DFB addition; on day 12 and day 21. . Bars are means of measurements in 3 independent mesocosms (n = 3) except for LC-DFB where n = 2. Error bars indicate SD.